International Journal of Applied Earth Observation and Geoinformation 139 (2025) 104545

Contents lists available at ScienceDirect

International Journal of Applied Earth Observation and Geoinformation

journal homepage: www.elsevier.com/locate/jag

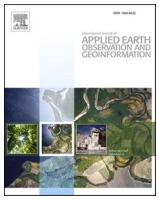

Spatially predicting ecosystem service patterns in boreal drained peatlands forests using multisource satellite data

Kaapro Keränen, Anwarul Islam Chowdhury, Parvez Rana *

Natural Resources Institute Finland (Luke), Helsinki, Finland

ARTICLE INFO

Keywords:
Satellite data
Optical image
Biodiversity
Ecosystem services
Carbon
Upscaling

ABSTRACT

Boreal drained-peatland forests provide diverse, interlinked ecosystem services (ESs), critical for informed decision-making in forest management. We mapped five ESs: bilberry yield, visual amenity, biodiversity conservation, carbon storage, and timber production using Landsat 8–9, Sentinel-2, and PlanetScope data. By combining these five ESs variables, we calculated a summed-ESs variable to capture overall ESs in drained peatland forests. Our objectives included assessing the influence of sensor resolution, auxiliary data, and the feasibility of scaling ESs predictions across varying canopy covers (closed, partial, and open). Using spectral bands and indices, we applied random forest regression, achieving explained variances (R^2) of 13–75 % for single ESs and 58–67 % for summed ESs. Sensor performance varied, with Landsat (R^2 22–69 %), Sentinel-2 (R^2 25–75 %), and PlanetScope (R^2 13–65 %). Incorporating auxiliary variables from seven-year-old LiDAR data improved model R^2 value by 1–24 %. We successfully scaled ESs predictions to map spatial distributions across the study area, with high ESs value in closed-canopy areas. These findings demonstrate satellite imagery's effectiveness for spatial ESs prediction, supporting sustainable drained-peatland forest management.

1. Introduction

Forest ecosystem services (ESs) represent the multitude of benefits that humans derive from the forest ecosystems (Brockerhoff et al., 2017). These services, essential to human well-being, include provisioning services such as timber, food production (Díaz-Yáñez et al., 2021), as well as regulating services like carbon storage, which play a critical role in mitigating climate change (Pukkala, 2016). These services also provide cultural benefits, including scenic and recreational value (MEA, 2005). Cultural services improve well-being by offering recreational areas, supporting both mental and physical health, and fostering a connection with the nature (Saarikoski et al., 2015). With increasing global demand, land-use changes, and biodiversity loss, the need for sustainable conservation and management of these essential services has become more increasingly important (Raudsepp-Hearne et al., 2010). Unfortunately, the world has seen over 60 % of ESs degradation, largely due to human interference and changing climate conditions (Raudsepp-Hearne et al., 2010; MEA, 2005). Despite being vital, ESs are often underappreciated in economic and policy decisions, primarily because of a lack of their status information, which causes unsustainable land use and environmental deterioration (Adegboyega et al., 2019).

In Finland, over 50 % (4.7 million hectare) of peatland are drained for forestry purpose. Drained peatlands forests provide berries (bilberry and cowberry), timber, carbon storage, biodiversity conservation, and visual amenity, which play a vital role in supporting both socio-economic and environmental well-being. Berries generate an annual harvest value of up to 115 million euros (Miina et al., 2009), significantly contributing to the national GDP. Berry-picking is a common activity for over half of the Finnish population (Peura et al., 2016), with most forests being accessible to the public under everyone's right, highlighting the cultural and social importance of this resource. The growing stock of Finnish boreal forests stands at 2475 million m3, and nearly 90 % of this is available for timber harvesting (Korhonen et al., 2021). Carbon storage, and biodiversity conservation hold significant importance. The visual amenity in Finland draws a significant number of visitors from around the world, supporting the tourism sector, while fostering a strong connection between people and nature.

Robust method are essential for assessment, and monitoring of peatland forests to ensure sustainable management (Korhonen et al. 2021). Various modelling approaches can be employed, including field data-based and remote sensing-based methods. Field data-based models

* Corresponding author.
E-mail address: parvez.rana@luke.fi (P. Rana).

https://doi.org/10.1016/j.jag.2025.104545
Received 17 November 2024; Received in revised form 22 March 2025; Accepted 16 April 2025
Available online 19 April 2025

rely on direct measurements and observations, providing detailed insights into specific forests area. In contrast, remote sensing-based models leverage satellite and aerial imagery to capture large-scale patterns and changes over time. Field data-based assessments of ESs often depend on National Forest Inventories (NFIs) and field surveys. While these methods provide accurate results, they are time-consuming, expensive, and limited in geographic scope (Fu et al., 2015). In ESs modelling based on field data, proxies such as tree diameter, dominant species, and growing stock are frequently employed (e.g., Ihalainen et al., 2002).

In recent decades, advancements in remote sensing have opened new possibilities for scalable and cost-effective modeling and assessment of ESs (Rana and Vauhkonen, 2023, Keränen et al. 2024, Hou et al. 2019). Remote sensing complements traditional field-based methods by capturing spatial and temporal variations in forests that may not be detectable through field surveys alone. Satellite remote sensing is extensively employed in ESs modelling, primarily for carbon storage, and timber production, and, to a lesser extent, non-timber forest products like berries, and visual amenity (but see Reich et al., 2018). Historically, medium-resolution sensors such as Landsat have been vital for providing long-term datasets essential for monitoring forests characteristics (Banskota et al., 2014). These datasets have proven particularly valuable for estimating carbon storage and timber by mapping forest structure and productivity across extensive regions. However, peatland forests present additional challenges, such as distinguishing between tree-covered and open peatland areas, subtle changes in canopy structure, and variations in understory vegetation such as berry-producing shrubs that often require higher spatial and temporal resolution and multi-source data. Recent high-resolution sensors like Sentinel-2 (10 m) and PlanetScope (3 m) offer more detailed spatial and temporal data (Alam et al. 2024), which could enhance the accuracy of ESs models for intricate, fine-scale issues such as berry yields and biodiversity conservation. Despite their promising capabilities, these sensors are still new, and their applications in ESs modelling are still limited.

Although satellite-based RS techniques offer valuable multispectral data for large-scale ecosystem monitoring, they do have limitations in specific ESs assessments, especially in situations where vertical structure is essential. Satellite data are highly effective for mapping surface-level attributes such as canopy cover changes (e.g., Roy et al., 2014) and struggles to penetrate dense vegetation or capture structural information. In contrast, LiDAR (Light Detection and Ranging) data provide three-dimensional insights into forest structure, including canopy height and tree density, which are crucial for precise estimations (e.g., Bohlin et al., 2021; Vauhkonen, 2018). However, LiDAR data collection is very costly, and many European Union (EU) countries planned to acquire LiDAR data every five to eight years intervals. Because of time difference between field data collection and LiDAR data acquisition, the direct use of LiDAR data in ESs inventory might be limited. However, LiDAR data could be useful as auxiliary data in addition to Satellite data. Therefore, utilizing LiDAR data can enhance the precision of satellite-based data ES models.

For forest managers, ESs maps can be a key reference source in decision-making for both forests resource management and conservation planning (Rana and Vauhkonen, 2023; Vauhkonen, 2018). They offer information about the status and distribution of each ESs. These maps play a crucial role in guiding land-use strategies for forest management while also aiding in pinpointing regions with significant ESs potential (Krsnik et al., 2023). ESs maps covering large areas are particularly valuable for supporting informed decisions in forest management, making them indispensable (Martínez-Harms and Balvanera, 2012; Vauhkonen and Ruotsalainen, 2017). ESs vary considerably across different canopy types, such as closed, partial, and open canopies (Felipe-Lucia et al., 2018). Management strategies favoring closed canopies and the conservation of old-growth broadleaved forests can enhance climate regulation services and cultural services, including the availability of edible fungi and culturally important plant species, while open canopies promote wild edible plants (Felipe-Lucia et al., 2018). This knowledge aids in prioritizing land-use strategies during forest management and helps identify areas with high ESs potential (Duarte et al., 2016; Krsnik et al., 2023; Vauhkonen and Ruotsalainen, 2017).

Satellites remote sensing enable autonomous, cost-effective mapping of ESs in peatland forests, but further exploration is needed with optical remote sensing data. A research gap remains regarding the impact of spatial resolution on prediction accuracy and the role of auxiliary data. To address this, we use remote sensing data from Landsat 8–9, Sentinel-2, and PlanetScope. We studied five ESs such as bilberry yield, visual amenity, biodiversity conservation, carbon storage, and timber production. By aggregating these ESs variables, we calculated a summed-ESs variable to capture overall ESs. To the best of our knowledge, no study has yet predicted a summed-ESs using multisource satellite data in drained peatland forests under different forest canopy covers, such as closed, partial and open. We evaluate the predictive accuracy of the sensors and develop a method to scale up field-based data with satellite imagery. Therefore, this study aimed to investigate: (1) the influence of sensor resolution on ESs prediction; (2) the contribution of auxiliary data to prediction accuracy; and (3) the feasibility of upscaling ESs predictions across different canopy covers, i.e., closed, partial and open canopy.

2. Materials and methods

2.1. Study area

The study was conducted in the Kivalo research forests of northern Finland (66°20′N 26°37′E) (Fig. 1). The total area of the study was 150 ha in drained-peatland forest. The study area was drained for forestry purposes in the 1930 s (Mäkiranta et al., 2012). The study area also included an old growth-forest conservation area. The study area contained research experimental areas for partial harvesting and control areas. The main tree species were Scots Pine (*Pinus sylvestris*), Birch (*Betula pendula*), and Norway Spruce (*Picea abies*). The study area was characterized by a mix of herb-rich type II and *Vaccinium myrtillus* type II vegetation. The average peat depths ranging from 30 to 90 cm (Minkkinen et al., 2007). The average effective temperature sum of 900-degree days (threshold of + 5°C) based on data from 1981 to 2010. The study area is famous for recreational use, and non-timber forests products (e.g., bilberry).

2.2. Field data

The field data was collected from Kivalo study area in summer 2023 (Table 1). The data was collected from 73 circular plots, with 9 m radius in each plot. We measured diameters of all trees with a diameter at breast height (DBH) over 5 cm. For each tree species within the plot, a tree with a DBH corresponding to the median tree was measured for height. These measurements were utilized to establish height curves for the prediction of missing height for other trees of the same species (Näslund, 1936). Volumes of individual trees were computed using species-specific equations (Laasasenaho, 1982), employing DBH and height as predictors. The volumes (V) of the trees were totalled at the plot level and scaled per hectare. In addition, the site type was recorded for each plot using Finnish site type classification (Cajander, 1909). We analysed the growth ring (1–2 per tree, depending on species and median DBH) to determine the age of tree in a plot. This involves counting the annual growth rings visible in a cross-section of the tree trunk. We used an increment borer tool to extract a core sample from the tree, allowing for ring counting without causing significant harm to the tree.

2.3. Ecosystem services calculation

Five ESs variables were calculated from the field measurements. Five ESs were bilberry yield (BILB), visual amenity (AMEN), biodiversity

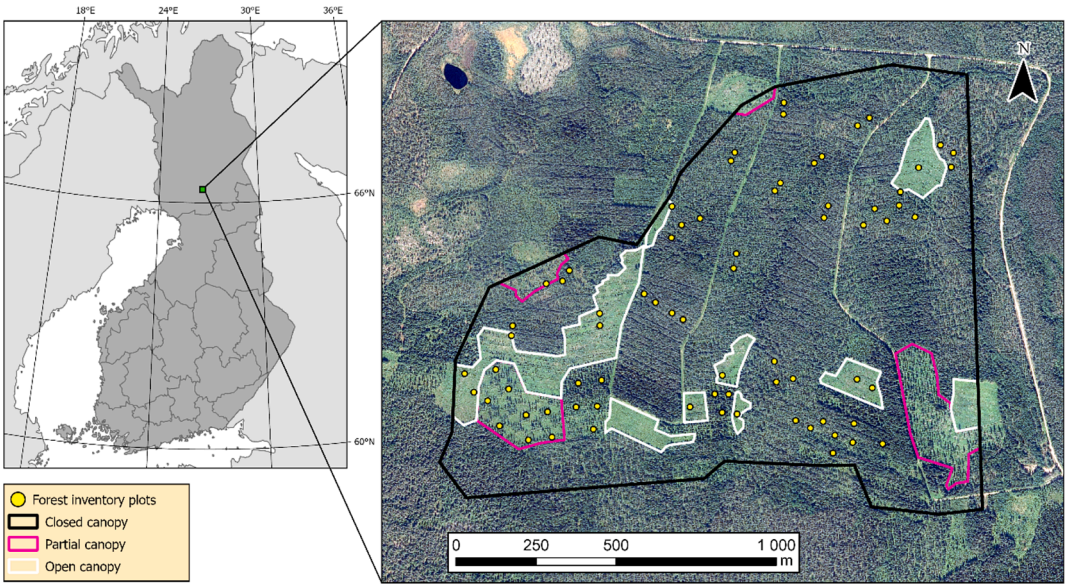

Fig. 1. Kivalo study area, forest inventory plots and their location portrayed. The forest treatment sites are bordered in the map.

conservation (BIOD), carbon storage (CARB) and timber production (TIMB). From the following five ESs variables, we calculated a summed ES variable (ES SUM) by combining them into single value to represent the overall ESs in the plots.

We calculated bilberry yields by Ihalainen et al., (2002) equation. Ihalainen et al., (2002) used tree age, height, basal area-weighted mean diameter, species-specific growing stock volume, basal area, and site fertility to calculate bilberry yield Eq. (1).

$$ln(V_b) = 0.0062t_g - 0.0136G + 0.0363h_{dom} + 0.0014V_p - 0.0013V_d - 0.2393D \quad (1)$$

where V_b is the bilberry yield, t_g the mean age of all trees (years) in each plot, G the basal area (m^2 /ha), h_{dom} the dominant height (m), V_p the volume of pine (m^3 /ha), V_d the volume of birch and other deciduous trees (m^3 /ha), D the dummy variable (D = 0, if forest site type is of *Myrtillus* type or more fertile; D = 1, if forest site type is of *Vaccinium* type or poorer) and d_g is the basal area weighted mean diameter of all trees (cm).

We used Pukkala et al. (1988) equation to calculate visual amenity. The age of the trees, diameter, volume of pine, birches, and other deciduous, and number of stems per hectare were used in the model Eq. (2).

$$B = 4.471 + 0.06450d_g - 0.0001745N + 0.006439V_pD + 0.005733V_bD \quad (2)$$

where B is visual amenity score, d_g is the basal area weighted mean diameter of all trees (cm), N is number of trees per hectare, V_p the volume of pine (m^3 /ha), V_b the volume of birches and other deciduous (m^3 /ha), D is 1, if dominant height >10 m and 0 otherwise.

We calculated biodiversity conservation value following Lehtomäki et al. (2015) which integrates forest inventory data to estimate conservation priorities. Specifically, the index is based on dominant tree species, mean diameter, total volume, and site fertility class. To quantify conservation value, Lehtomäki et al., (2015) assigned expert-derived weights to different tree species groups based on their ecological importance. Deciduous species, particularly in old-growth forests, were given higher scores due to their association with high biodiversity values. More fertile sites were prioritized, as they support diverse vegetation and associated species communities. The calculation followed a sigmoidal benefit function, where increasing tree diameter and volume contributed non-linearly to the conservation value, ensuring that mature forests with high structural complexity received the highest rankings. For biodiversity conservation, in the absence of detailed plant mapping data, we used proxy values derived from forest inventory data. To our knowledge, no alternative functions better capture biodiversity conservation in this specific context than those proposed by Lehtomäki et al. (2015).

We calculated the above-ground carbon storage by multiplying the total volume of each species by a specific conversion factor (Karjalainen and Kellomäki, 1995) where the total volume of species of each plot was calculated by species-specific equation (Laasasenaho, 1982).

$$C = 0.3091V_p + 0.3715V_s + 0.4152V_d \quad (3)$$

where C is total carbon storage, V_p the volume of pine (m^3 /ha), V_s the volume of spruce (m^3 /ha), and V_b the volume of birches and other deciduous (m^3 /ha).

We used the soil expectation value (SEV) for timber production following the suggestion from Rana and Vauhkonen (2023), Vauhkonen, (2018). SEV represents the present value (€/ha) of all costs and revenues associated with timber production, assuming perpetual forest management rotations (Vauhkonen, 2018). SEV incorporate variables such as site fertility, growing stock, and operational factors (e.g., temperature, interest rates, timber prices) (Pukkala, 2005). In our study area, the effective temperature sum was 900-degree days. SEVs were computed using average interest rates ranging from 1 % to 4 %, coupled with various combinations of saw-wood/pulpwood prices (€/m^3): 30/15, 30/25, 40/15, 40/25, 40/35, 50/25, and 50/35.

Although multiple modeling approaches were available to estimate individual ESs values, the selected models were rigorously validated in previous studies (Turtiainen, 2015; Silvennoinen, 2017; Rana and Vauhkonen, 2023), which demonstrated that alternative models would not enhance the relevance of the results.

We normalized the individual ESs values before calculating summed ESs values. The objective of data normalization is to standardize values of ESs onto a common scale for facilitating easier comparison and analysis of ESs. For normalizing ESs values, we used box-cox transformation, proposed by Box and Cox (1964), to normalize the value of ESs by using the R package *bestNormalize*. The ESs is ratio-scaled between 0–1 values by following Vauhkonen (2018). This technique offers the benefit of defining clear boundaries, ensuring that all ESs share a consistent range between 0 and 1.

Table 1
Forest inventory data summary (n = 73), closed canopy (n = 53), partial canopy (n = 9), open canopy (n = 11). A closed canopy forest has dense, overlapping tree crowns (>70 % cover). A partial canopy forest has moderate cover (40–70 %), with some gaps between crowns. An open canopy forest has sparse tree cover (<40 %), with significant gaps (Jennings et al., 1999).

Attributes		Mean	Min	Max
Diameter, cm	Closed canopy	16.46	9.74	34.62
	Partial canopy	14.19	5.07	26.43
	Open canopy	7.15	5.18	11.85
Dominant height, m	Closed canopy	12.58	7.62	20.57
	Partial canopy	10.33	3.60	16.95
	Open canopy	5.19	3.74	7.72
Basal area, m^2/ha	Closed canopy	20.11	6.48	55.09
	Partial canopy	7.67	0.13	13.18
	Open canopy	0.59	0.17	1.38
Basal area weighted mean diameter, cm	Closed canopy	23.22	15.07	41.99
	Partial canopy	18.90	5.14	33.99
	Open canopy	5.31	5.32	11.85
Above ground biomass, ton/ha	Closed canopy	85.19	31.68	266.20
	Partial canopy	30.18	0.31	59.39
	Open canopy	1.58	0.43	3.95
Total volume, m^3/ha	Closed canopy	152.81	52.09	472.23
	Partial canopy	51.48	0.34	94.55
	Open canopy	2.07	0.45	5.98
Pine, m^3/ha	Closed canopy	80.74	0	212.17
	Partial canopy	20.89	0	70.98
	Open canopy	0	0	0
Spruce, m^3/ha	Closed canopy	45.96	0	343.91
	Partial canopy	20.35	0	75.09
	Open canopy	1.51	0	4.02
Deciduous, m^3/ha	Closed canopy	26.11	0	94.12
	Partial canopy	10.24	0	39.11
	Open canopy	0.56	0	2.38
Age, years	Closed canopy	64	16	133
	Partial canopy	60	39	95
	Open canopy	23	8	54
Number of trees/ha	Closed canopy	954	117	2004
	Partial canopy	489	39	1493
	Open canopy	149	39	353

$$E_{ij} = \frac{ES_{ij} - min(ES_i)}{max(ES_i) - min(ES_i)} \quad (4)$$

where E_{ij} is the normalized value of i^{th} ES in plot j, ES_{ij} is the actual value of ES, min (ES_i) the minimum value and max (ES_i) the maximum value of all plots.

2.4. Remote sensing data

We acquired cloud free optical satellite data from the July of 2023. We used optical satellite data from three different spatial resolution (Fig. 2). The satellite imagery data is atmospherically corrected data from Landsat 8–9 (NASA/USGS), Sentinel-2 (ESA) and PlanetScope (Planet Inc.). The spatial resolutions for the corresponding satellites are 30 m, 10 m, and 3 m, respectively. Spectral wavelength bands blue, green, red, near-infrared (NIR), shortwave infrared (SWIR) 1 and 2 were downloaded from the imagery of Landsat 8–9 and Sentinel-2. For the PlanetScope, the SWIR data was not available, but otherwise the bands were same. In addition to optical satellite data, we used available auxiliary datasets. In our study area, light detection and ranging (LiDAR) data was also acquired from seven years ago (2016) which were available with a point density of 0.5p/m^2.

2.5. Feature extraction

We extracted individual spectral bands, multiple vegetation indices and moisture-related indices from optical satellite data (Table 2). The indices were selected based on their correlations with vegetation and biomass distribution. We calculated vegetation indices due to their strong correlated with vegetation greenness (Rana 2016, Rana et al. 2023), while moisture-related indices were selected for their surface wetness in drained-peatlands forests (Keränen et al. 2024) When a sample plot polygon extended across multiple raster pixels, the area-weighted mean of individual spectral bands and indices was calculated within each plot to ensure consistency in feature extraction.

In addition to optical data, we extracted 10 variables from LiDAR data. The variables were related to tree height, density and understory vegetation (Table 2). Recent studies have employed these variables in forest structure analyses (e.g. Rana and Vauhkonen 2023; Rana et al. 2023). The first echoes included the categories "*first of many*" and "*only*", while the last echoes consisted of "*last of many*" and "*only*". These first and last echoes provided the structural information about the upper and lower canopy layers (Rana & Vauhkonen, 2023; Rana, 2016). Additionally, the selection of a threshold value for LiDAR variable extraction was based on established methodologies from previous research (e.g., Rana et al. 2016; Rana et al., 2023).

2.6. Regression model

We constructed random forest regression models (Breiman, 2001) for predicting the ESs values. The remote sensing data derived bands and indices was used as the predictor variables and ESs variables calculated from the field measurements were the response variables. Random Forest was chosen due to its ability to handle high-dimensional data, capture complex non-linear relationships, and provide robust predictions without requiring assumptions about data distribution. Compared to other machine learning approaches, Random Forest offers advantages in terms of computational efficiency and reduced sensitivity to hyperparameter tuning, making it well-suited for remote sensing applications. Its effectiveness in handling remote sensing data with multiple variables as proven by earlier corresponding studies (Purohit et al., 2021; Isoaho et al., 2024; Keränen et al., 2024). Further, the random forest can build models while not having requirements for predictor variables' multi-collinearity and not suffering from overfitting the model (Belgiu and Drăguţ, 2016).

We built separate models using the spectral data of three different satellite sensors: Landsat 8–9, Sentinel-2 and PlanetScope to compare their predictive capacities. For models of Landsat and Sentinel there were 16 predictor variables, whereas 11 predictors for the PlanetScope model (Table 2). We made six models for each sensor, to predict the values of five individual ES variables and the summed ES variable. Additionally, we added auxiliary LiDAR data consisting of 10 variables for each optical sensor model to improve the prediction accuracies. As the auxiliary data was added to the modelling of individual ES variables, we constructed 36 models in total. To evaluate model performance, we used the Kolmogorov-Smirnov (K-S) test to assess whether the predicted values follow the same distribution as observed data. Additionally, we employed the Kruskal-Wallis test to assess whether the predicted values

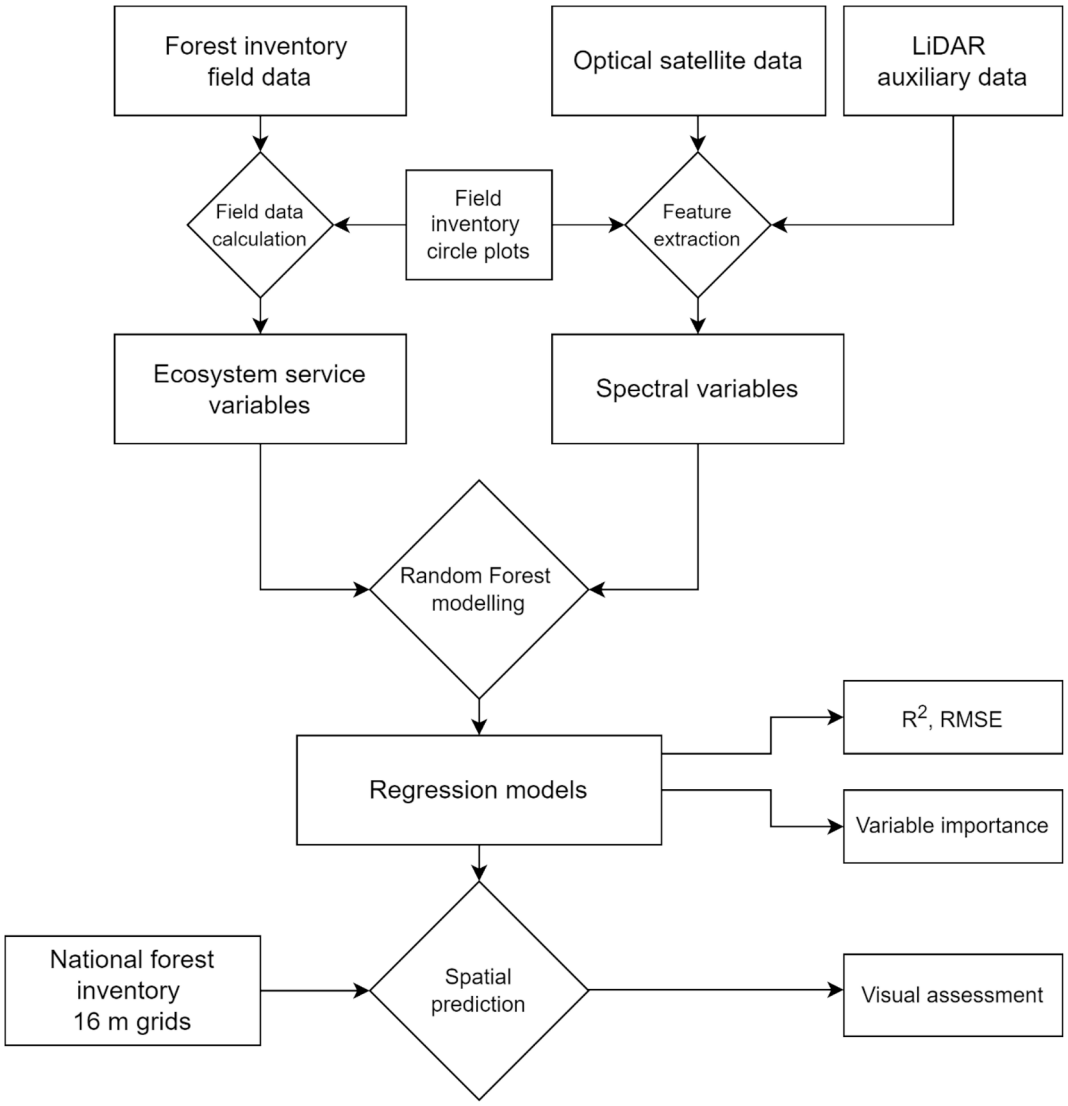

Fig. 2. Flowchart summarizing the methodology employed in this study. LiDAR: light detection and ranging, R^2: percentage of variance explained and RMSE: root-mean-square error.

of ESs differed significantly across closed, open, and partial canopy cover.

The models were built within the *Caret* package and assessed by 10-fold cross-validating the data. We ended up using the default parameters of 500 trees and one third (1/3) of tries at every split for the dataset, based on our initial testing and because the default settings produce sufficiently accurate models. The final model accuracies were estimated by the percentage of variance explained by the model (R2) and by root-mean-square error (RMSE) percentage values normalized by the average RMSE value. In addition to regression models, we conducted variable importance analysis for ESs variable models using only optical sensor data. The variable importance values were extracted from the regression models and scaled 0–100 summing up to 100 with all spectral variables' importance per each ESs variable modelling.

2.7. Upscaling to larger areas

Finally, the models based on circular plots were predicted spatially on the whole study area of Kivalo site. The spectral values were first extracted inside 16 m resolution grids based on National Forest Inventory grid of Finland. We then computed the area-weighted mean for each band and index within these grids. Grid containing roads were excluded from the predictions. To get comparison between sensor accuracies and spatial differences of the ESs variables, we used models based on optical satellite data. These models were predicted to the 16 m grids and the results were evaluated through visual assessment. ArcGIS Pro (version 2.7.0) was used for map visualization to enhance spatial interpretation.

3. Results

3.1. Different sensors for ecosystem services prediction

All sensors yielded accurate results, with notable differences in performance across Landsat (R^2 = 22–69 %, RMSE = 29–42 %), Sentinel-2 (R^2 = 25–75 %, RMSE = 26–40 %), and PlanetScope (R^2 = 13–65 %, RMSE = 31–44 %) (Fig. 3). Our results indicate that models using Sentinel data were the most accurate for predicting ESs variables. Models with Landsat and PlanetScope data showed comparable performance, though some differences in accuracy were observed across ESs variable models for each sensor. However, the accuracy of predictions varied significantly between ESs variables.

Carbon storage was modeled with the highest accuracy, with R^2 values ranging from 65 % to 75 % and RMSE values between 27 % and

Table 2
List of variables calculated from the Landsat 8–9, Sentinel-2, PlanetScope and LiDAR data.

RS variable	Abbreviation	Formula	Reference
Blue band	Blue		
Green band	Green		
Red band	Red		
Near-Infrared band	NIR		
Shortwave Infrared 1 *	SWIR 1		
Shortwave Infrared 2 *	SWIR2		
Normalized Difference Vegetation Index	NDVI	$\frac{NIR - Red}{NIR + Red}$	(Rouse et al., 1974)
Normalized Difference Water Index	NDWI	$\frac{Green - NIR}{Green + NIR}$	(McFeeters, 1996)
Enhanced Vegetation Index	EVI	$2.5 \times \frac{NIR - Red}{NIR + 6 \times Red - 7.5 \times Blue + 1}$	(Liu & Huete, 1995)
Soil Adjusted Vegetation Index	SAVI	$1.5 \times \frac{NIR - Red}{NIR + Red + 0.5}$	(Huete, 1988)
Normalized Difference Phenology Index *	NDPI	$\frac{NIR - (0.74 \times Red + 0.26 \times SWIR1)}{NIR + (0.74 \times Red + 0.26 \times SWIR1)}$	(Wang et al., 2017)
Normalized Difference Tillage Index *	NDTI	$\frac{SWIR1 - SWIR2}{SWIR1 + SWIR2}$	(Daughtry et al., 2010)
Green Normalized Difference Vegetation Index	GNDVI	$\frac{NIR - Green}{NIR + Green}$	(Gitelson et al., 1996)
Green-Red Vegetation Index	GRVI	$\frac{Green - Red}{Green + Red}$	(Motohka et al., 2010)
Optimized Soil Adjusted Vegetation Index	OSAVI	$\frac{NIR - Red}{NIR + Red + 0.16}$	(Rondeaux et al., 1996)
Normalized Difference Infrared Index *	NDII	$\frac{NIR - SWIR}{NIR + SWIR}$	(Hardisky et al., 1984)
LiDAR	Diff_fplp	Mean height difference between first echo and last echo	(Liang et al., 2007)
	Diff_only_lp	Mean height difference between only echoes and last echoes	(Liang et al., 2007)
	Diff_only_fp	Mean height difference between only echoes and first echoes	(Liang et al., 2007)
	D10_lp	Proportional densities at the 10th percentile for the last echoes	(Næsset, 2002)
	D95_fpm	Proportional densities at the 95th percentile for the first of many echoes	(Næsset, 2002)
	Hstd_fp	Standard deviation of height for the first echoes	(Næsset, 2002)
	Hstd_lp	Standard deviation of height for the last echoes	(Næsset, 2002)
	Prop_fp	Proportion of first echoes to all echoes	(Rana and Vauhkonen 2023)
	Vegrat_fp	Proportion of first echoes above 0.5 *m*	(Korhonen et al., 2008)
	Vegrat_fpm	Proportion of first of many echoes above 0.5 *m*	(Korhonen et al., 2008)

* Available only for Landsat 8–9 and Sentinel-2.

31 %. The next best models were for visual amenity and biodiversity. Visual amenity models achieved moderate R^2 values (42–50 %), though their RMSE values were the highest among ES variables (40–44 %). Biodiversity models exhibited lower R^2 values (35–50 %) but better RMSE values (32–36 %) compared to visual amenity. Bilberry picking showed distinctly lower accuracy, with R^2 values of 22–31 % and RMSE values of 35–37 %. Timber production models were the least accurate in terms of R^2 (13–26 %), yet RMSE values (35–38 %) were relatively favorable compared to other ES variable models.

Modelling of the summed ESs variable produced similar accuracy order for all three sensors, with Sentinel being the most accurate (R^2 68 %, RMSE 25 %), PlanetScope the second most accurate (R^2 63 %, RMSE 27 %) and Landsat the least accurate (R^2 58 %, RMSE 29 %). The predicted values followed the same distribution as observed data as indicated by the Kolmogorov-Smirnov ($p > 0.05$). However, the predicted values of ESs differ significantly across closed, open, and partial canopy cover, based on Kruskal-Wallis ($p < 0.05$).

The variable importance analysis showed consistent results across all sensors (Fig. 4). Single bands emerged as the most important predictors in all models, particularly the green and SWIR bands. Among indices, EVI, SAVI, and OSAVI stood out as the most influential variables.

3.2. Models with auxiliary old LiDAR data

The model accuracies improved after the addition of old LiDAR data. All the ESs variable model accuracies from each sensor improved within similar way (Fig. 3). The models' R2 increased within the range of 1–24 %. Respectively, the RMSE values decreased consistently for all models by 1–6 %.

3.3. Upscaling to larger areas

Applying the regression models across the entire 16 m gridded study area produced realistic spatial patterns. Sentinel and PlanetScope provided more accurate spatial representations compared to Landsat. The highest ES values across all individual ESs were predicted within closed canopy areas, while the lowest values appeared in open canopy areas (see Fig. 1; Fig. 5). This distinction was especially clear when visually comparing the predicted maps with canopy covers in aerial *ortho*-imagery (see Fig. 1 and Fig. 5).

Predictions for visual amenity, biodiversity, and carbon storage exhibited the greatest contrast between high and low values within closed and open canopy areas. Spatial modeling of the summed ESs variable demonstrated that areas with high ESs values consistently aligned with closed canopy areas, whereas areas with low ESs values corresponded to open canopy areas.

4. Discussion

Our study reveals that ESs can be accurately predicted by integrating field data with regression models based on medium to high spatial resolution optical satellite imagery (3–30 m). However, variations in model performance were evident between different satellite sensors and specific ESs variables. Furthermore, ESs values showed distinct differences between various canopy cover types.

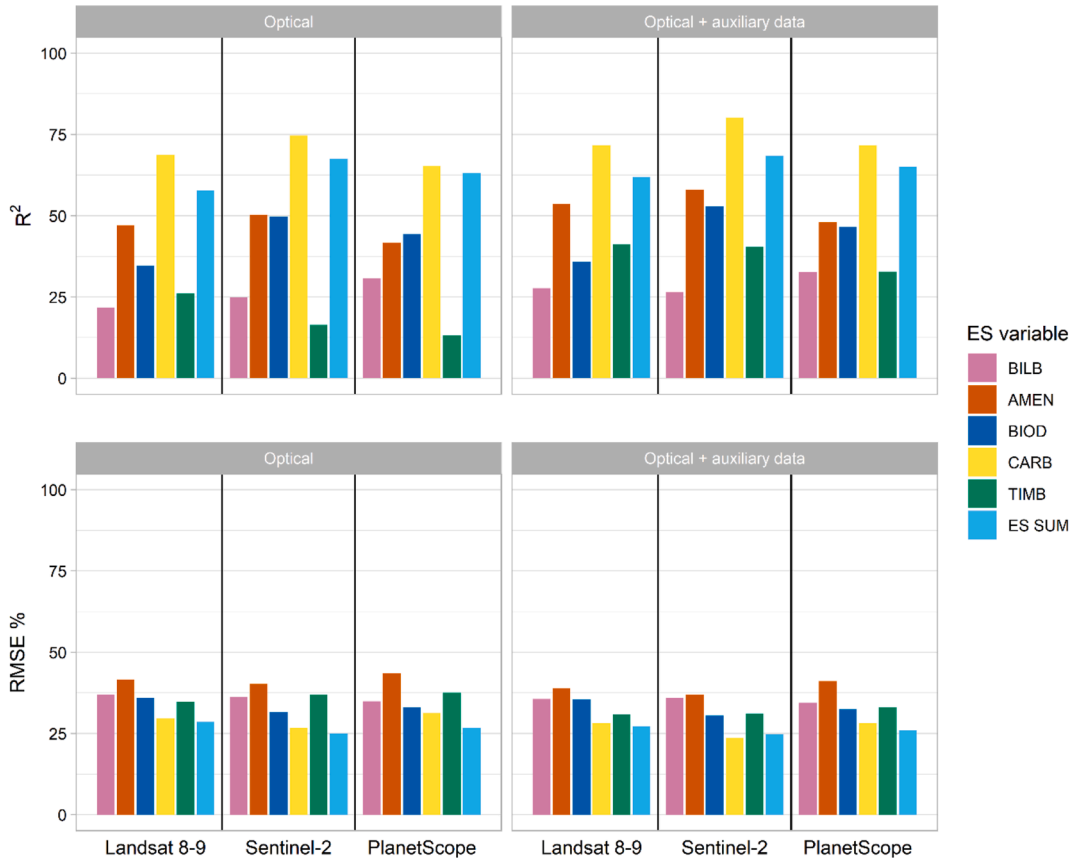

Fig. 3. Random forest regression model accuracies for ecosystem services (ESs) such as bilberry yield (BILB), visual amenity (AMEN), biodiversity conservation (BIOD), carbon storage (CARB) and timber production (TIMB), summed ES variable (ES SUM). Auxiliary data includes seven years old LiDAR data.

4.1. Effects of spatial and spectral resolution of remote sensing data

Spatial resolution affects the predictive accuracy of various ESs (Coops et al., 2023). High-resolution imagery from sensors such as Sentinel-2 and PlanetScope demonstrated greater accuracy in assessing ESs compared to coarser resolution imagery (30 m) from Landsat 8–9. However, compared to Planetscope and Landsat, Sentinel-2 offers higher radiometric quality, which improves the predictive performance of models (Räsänen et al., 2021). Despite its lower spatial resolution compared to Planetscope, Sentinel-2 compensates with higher spectral resolution, particularly its strategically positioned SWIR bands, which enhance accuracy in assessments of ESs like carbon storage, timber production, and biodiversity conservation (Astola et al., 2019; Chraibi et al., 2022; Korhonen et al., 2017; Puliti et al., 2021; Wang et al., 2022). Sentinel-2′s frequent revisits and better radiometric quality also make it more suitable than Planetscope, which suffers from a lower signal-to-noise ratio, particularly in shortwave infrared bands and under variable atmospheric conditions (Houborg & McCabe, 2018). This limitation can introduce spectral inconsistencies, reducing the reliability of PlanetScope data for detecting subtle ecosystem variations. Several studies (e.g., Kluczek et al. 2023; Pacheco-Prado et al. 2024) reported the higher performance of Sentiel-2 than PlanetScope data in ESs mapping. However, there is a contradiction in various studies (Acharki, 2022), where PlanetScope was found to outperform both Sentinel-2 and Landsat 8–9 in terms of accuracy. For instance, Gašparović et al. (2018) reported a higher accuracy of PlanetScope than Sentinel-2 imagery for vegetation detection and monitoring. Additionally, Landsat 30-meter spatial resolution can smooth out smaller-scale heterogeneity, making it less effective for capturing fine-grained ESs variations, such as those associated with understory vegetation (Wulder et al., 2019).

Spectral proxies have proven to be powerful variables for characterizing ESs, offering detailed insights into various vegetation structures and health indicators. The results of our study align with previous research, which has demonstrated the effectiveness of spectral indices in estimating ESs. Our findings, particularly the strong performance of single bands, and vegetation indices like EVI, SAVI, and OSAVI, are consistent with the several studies (e.g., Giannetti et al., 2018; Korhonen et al., 2017; and Zhang et al., 2023). These studies have also highlighted the utility of these indices in biomass estimation, forest health monitoring, and species classification. A study by Qiu et al. (2020) demonstrated that green variance and SWIR variance derived from Landsat-8 imagery are strongly correlated with biomass, supporting the findings of our study. The prominence of vegetation index in our study is further supported by John et al. (2018), who emphasized its sensitivity to vegetation canopy structure and photosynthetic activity. Moreover, studies by Erdenebaatar et al. (2021); Nakano et al. (2013); identified that soil-related indices, such as SAVI and OSAVI, are highly relevant for estimating AGB and carbon stock.

In our study, auxiliary LiDAR data provided structural information on forest attributes, which complemented the ES model and improved its accuracy. Structural information is crucial for ESs prediction, as our expert model relies heavily on forest structural attributes such as height, DBH, and growing stock. Several studies have shown that incorporating structural data can significantly improve predictive model accuracy (Jiang et al., 2022; Pope and Treitz, 2013; Shen et al., 2019). For example, Shen et al. (2019) investigated that considering structural proxies alongside spectral proxies, can reduce the average RMSE by up to 8 % for forest stand volume prediction. Nevertheless, LiDAR data can provide detailed understory vegetation information. This combined approach enhances the predictive power of ESs models by leveraging the strengths of each data type, leading to better performance in predicting ESs (Jiang et al., 2022; Lu et al., 2016).

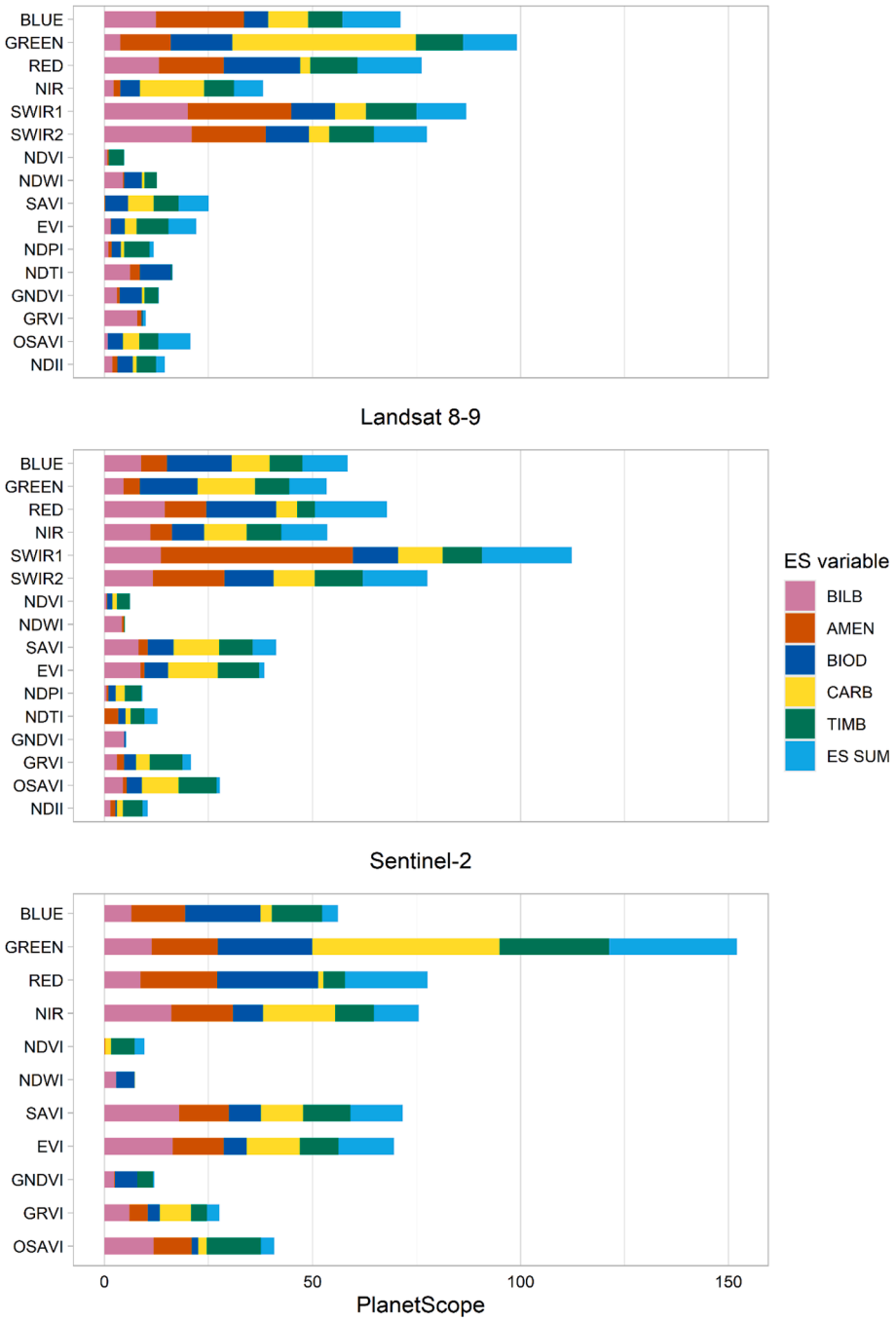

Fig. 4. Variable importance of the optical variables from models with only optical sensor data. Ecosystem services (ESs) variables such as bilberry yield (BILB), visual amenity (AMEN), biodiversity conservation (BIOD), carbon storage (CARB) and timber production (TIMB), and summed ES variable (ES SUM).

4.2. Ecosystem services regression model performance

The prediction of bilberry yield estimation using satellite data is still limited. The estimated bilberry yield reported by Reich et al. (2018) in Port Graham, Alaska, using Landsat 8 data achieved an impressive accuracy of R^2 values ranging from 73 % to 96 %, which surpasses the accuracy of our results. Their study employed a generalized linear model that incorporated 25 independent variables to predict production and abundance. In contrast, Vauhkonen (2018) developed bilberry models for boreal peatlands using airborne LiDAR data, achieving accuracy levels comparable to those of our bilberry model (R^2 = 22–31 % and RMSE = 35–37 %). Additionally, a study by Bohlin et al. (2021) in Sweden integrated LiDAR data with auxiliary information from the National Forest Inventory, reporting an R2 value of 40 %, which is higher than our bilberry model's accuracy. One limitation of using spectral proxies is that they provide only limited understory vegetation information, particularly regarding the presence of shrubs, which is crucial for estimating bilberry yields. By incorporating LiDAR data as auxiliary information, we observed an improvement (R^2 = 2–5 % and RMSE = 2–3 %) in the accuracy of our predictive bilberry models. Some studies (e.g., Vauhkonen, 2018; Vauhkonen and Imponen, 2016) mentioned that ALS pulses can penetrate the canopy of forest stands, capturing crucial ground information especially the presence of shrubs and understorey, which enhances the accuracy of berry predictions. Moreover, future studies could explore the climate variable in modeling to improve the model performance (Kilpelläinen et al. 2016).

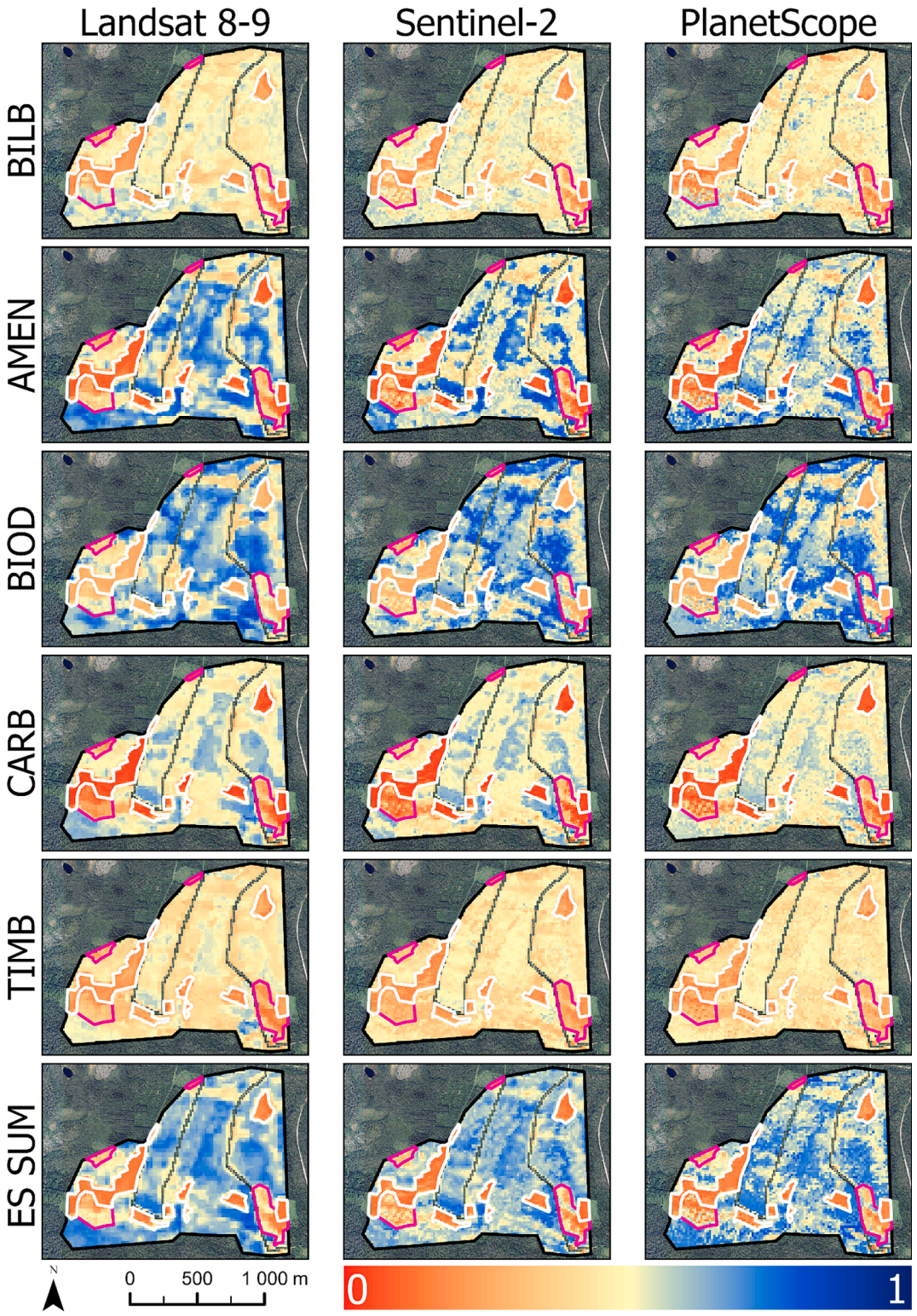

Fig. 5. Spatial predictions of ecosystem services (ES) values from regression models. ESs such as bilberry yield (BILB), visual amenity (AMEN), biodiversity conservation (BIOD), carbon storage (CARB) and timber production (TIMB), summed ES variable (ES SUM). The pixels with road were excluded from the spatial modelling. The forest treatment site borders are the same as in Fig. 1.

There are few studies on visual amenity prediction using optical imagery. According to the expert model used in our study, visual amenity is mostly related to the types of species present in the stand. Specifically, visual amenity correlates strongly with the size and age of trees, as well as the proportion of pines and birches (Pukkala et al., 1988). Conversely, stands with small trees tend to have lower visual amenity scores, and areas that are partially cut or clear-cut are associated with reduced visual amenity potential (Savolainen and Kellomaki, 1981). In our study, spectral information, particularly various indices, provided valuable insights into tree species and canopy characteristics, significantly enhancing the accuracy of our visual amenity potential predictions. However, several studies employed forest stand

characteristics to score the visual amenity (Pukkala et al., 1988; Vauhkonen, 2018). However, other studies also considered the landscape characteristics (Schirpke et al., 2013), and individual people preferences (Jia et al., 2022; Wang et al., 2020). Using LiDAR data, Vauhkonen (2018) predicted visual amenity based on forest stand characteristics for the southern boreal forest in Finland, achieving a RMSE value of 22 % to 28 %, which is lower than our RMSE (40–44 %).

There are several studies focusing on biodiversity conservation using satellite data. In our study, the biodiversity conservation model achieved reasonable accuracy, largely due to the strong dependence of biodiversity conservation on species composition and stand structure. For instance, Hoffmann et al. (2022) applied deep neural network regression to assess structural diversity in north-eastern Germany, achieving an RMSE of 33 % with Sentinel-1 and Sentinel-2 data. Liu et al. (2023) demonstrated that the combination of Sentinel-1 and Sentinel-2 imagery can effectively predict species richness, yielding an R^2 of 56 % when using heterogeneity metrics, non-heterogeneity metrics, and topographic variables. Our results indicated a slightly lower R^2 range (35–50 %) but achieved more favourable RMSE percentages (31–36 %), suggesting stronger predictive reliability.

Our findings consistently align with the accuracy and efficiency of regression models for predicting carbon storage reported in several studies. For instance, Puliti et al. (2021) observed similar accuracy in estimating above-ground biomass (AGB, which can be used as a proxy for carbon) in southeastern Norway using Sentinel-2 and Landsat data. In our study, the carbon estimation accuracy improved further with the addition of LiDAR data, reducing the RMSE by up to 7 %. This is consistent with the findings of Jiang et al. (2022), who reported a RMSE of 46 % when using LiDAR and Sentinel-2 data together, compared to 58 % when using only Sentinel-2 data. Moreover, Räsänen et al. (2021) reported comparable accuracy in their study conducted in Eurasia and North America, utilizing Sentinel-2 and PlanetScope data, with R^2 ranging from 36 % to 70 %.

Timber production models were the least accurate, largely due to the complexity of the factors involved in estimation. Several key reasons contribute to this limited accuracy, including dependency on site fertility, meteorological variables like temperature, and economic factors such as interest rates. This information is crucial for accurately estimating timber production but are challenging to assess through remote sensing data alone. Astola et al. (2021) conducted a study in Central Finland using Sentinel-2 data to estimate timber volume stock, achieving a similar accuracy with an RMSE of 31 %. Tuominen et al. (2017) reported a significantly higher RMSE of 60 % in Central Finland, suggesting our model provides substantially better predictive accuracy in estimating timber production. Wittke et al. (2019), however, achieved a lower RMSE of 27 % in Southern Finland using Sentinel-2 data. In our study, we calculated summed-ESs using a straightforward approach. However, trade-offs between multi-ESs are possible (Rana and Vauhkonen 2023). For instance, the shift towards monoculture plantations, where a single tree species is cultivated extensively, can further exacerbate biodiversity loss. While these plantations are efficient for timber production, they often lack the structural complexity and species diversity of natural forests, making them less resilient to pests, diseases, and environmental changes (Liu et al. 2018). Moreover, future studies could explore the weighted approaches for calculating summed-ESs.

4.3. *Upscaling for forest management support*

The spatial upscaling in this study was successful for all ESs and sensor types, as evident in the ESs patterns when compared to the orthoimage. Closed canopy areas are more favourable for ESs compared to partial and open canopies, likely due to their greater biomass, microclimatic stability, and carbon sequestration potential (Pukkala, 2016; Felipe-Lucia et al., 2018). In contrast, Open canopy areas with few trees demonstrate low ESs values throughout the study area (Felipe-Lucia et al., 2018). While closed-canopy forests maximize carbon storage and timber yield, they may also limit the availability of certain non-timber forest products, such as berries, which tend to thrive in more open conditions with higher light penetration (Gamfeldt et al., 2013). Similarly, biodiversity outcomes may vary; although closed-canopy stands provide habitat for shade-tolerant species, more open canopies can support greater plant diversity and structural heterogeneity, which benefit pollinators and understory flora (Felipe-Lucia et al., 2018). ESs maps are crucial tools for forest managers, as they provide critical insights into the spatial distribution of ESs (Mononen et al., 2017). Different spatial resolutions of ESs maps can significantly influence management decisions, as they offer varying levels ESs. Sentinel-2 or PlanetScope derived ESs maps are useful to capture subtle variations in ESs. Moreover, the ability to visualize the distribution of ESs across different canopy cover can aid forest managers in prioritizing areas for conservation or restoration efforts (Vauhkonen and Ruotsalainen, 2017; Felipe-Lucia et al., 2018). The detailed maps generated in this study allow for targeted interventions that can enhance specific ESs. By integrating ESs maps into management practices, forest managers can better align their strategies with both ecological objectives and socio-economic needs (Orsi et al., 2020). Furthermore, the methodology applied in this study could be extended to similar forest types and geographical regions, providing a scalable approach for assessing ESs in different landscapes. Furthermore, these spatial maps can support stakeholder engagement by providing clear visual representations of ESs that can be communicated to the stakeholders and decision-makers (Klein et al., 2015). By highlighting areas of high ESs potential, these maps can help in sustainable forest management practices and conservation initiatives. Moreover, future studies could explore the integration of multi-sensor approaches including drone data or the inclusion of auxiliary variables, such as climatic variable, particularly in the context of climate change and long-term forest sustainability.

5. Conclusion

This study evaluated three optical satellite products for predicting ESs and assessed the influence of spatial and spectral resolution on predictive performance. The findings revealed that while all three satellite image sensors achieved good accuracy in ESs prediction, PlanetScope and Sentinel-2 outperformed Landsat. Furthermore, incorporating older auxiliary LiDAR data enhanced model performance. Key conclusions from our study are as follows:

- Among the predicted ESs, carbon storage exhibited the highest prediction accuracy, highlighting its strong correlation with spectral and structural forest attributes.
- Summing multiple ESs provided a more comprehensive spatial representation, reducing the limitations associated with individual ESs predictions and offering a holistic perspective on ecosystem functionality.
- During upscaling to larger areas, the ESs maps demonstrated realistic spatial patterns, reinforcing their reliability for decision-making.
- Canopy structure significantly influenced ESs distribution, with closed-canopy areas showing consistently higher ESs values compared to partial and open canopies.
- These spatial ESs maps can support stakeholder engagement by providing clear, visual representations that facilitate communication with stakeholders and decision-makers.

Overall, the developed methodology is highly applicable for mapping multiple ESs in boreal drained peatland forests, offering a scalable approach for ecosystem monitoring and sustainable management.

Funding sources

This study was funded by Horizon Europe project ALFAwetlands (Grant Agreement Number 101056844).

CRediT authorship contribution statement

Kaapro Keränen: Writing – review & editing, Writing – original draft, Visualization, Validation, Software, Methodology, Formal analysis, Data curation. **Anwarul Islam Chowdhury:** Writing – review & editing, Writing – original draft, Resources, Methodology, Data curation. **Parvez Rana:** Writing – review & editing, Writing – original draft, Visualization, Validation, Supervision, Resources, Project administration, Methodology, Funding acquisition, Conceptualization.

Declaration of competing interest

The authors declare that they have no known competing financial interests or personal relationships that could have appeared to influence the work reported in this paper.

Acknowledgment

The authors wish to acknowledge Pekka Närhi, Eemeli Sarajärvi, Priscillia Christiani, Mauri Heikkinen, Hannu Herva, Jukka Lahti for helping the field data collection.

Data availability

Data will be made available on request.

References

Acharki, S., 2022. PlanetScope contributions compared to Sentinel-2, and Landsat-8 for LULC mapping. Remote Sens. Appl.: Soc. Environ. 27, 100774.
Adegboyega, S.A., Oloukoi, J., Olajuyigbe, A.E., Ajibade, O.E., 2019. Evaluation of unsustainable land use/land cover change on ecosystem services in coastal area of Lagos state, Nigeria. Appl. Geomat. 11, 97–110.
Alam, M.M.T., Simic Milas, A., Gašparović, M., Osei, H.P., 2024. Retrieval of crop canopy chlorophyll: machine learning vs radiative transfer model. Remote Sens. 16 (12), 2058.
Astola, H., Häme, T., Sirro, L., Molinier, M., Kilpi, J., 2019. Comparison of Sentinel-2 and Landsat 8 imagery for forest variable prediction in boreal region. Remote Sens. Environ. 223, 257–273.
Banskota, A., Kayastha, N., Falkowski, M.J., Wulder, M.A., Froese, R.E., White, J.C., 2014. Forest monitoring using landsat time series data: a review. Can. J. Remote. Sens. 40, 362–384. https://doi.org/10.1080/07038992.2014.987376.
Belgiu, M., Drăguţ, L., 2016. Random forest in remote sensing: a review of applications and future directions. ISPRS J. Photogramm. Remote Sens. 114, 24–31.
Bohlin, I., Maltamo, M., Hedenås, H., Lämås, T., Dahlgren, J., Mehtätalo, L., 2021. Predicting bilberry and cowberry yields using airborne laser scanning and other auxiliary data combined with National Forest Inventory field plot data. For. Ecol. Manage. 502, 119737.
Breiman, L., 2001. Random forests. Mach. Learn. 45, 5–32.
Brockerhoff, E.G., Barbaro, L., Castagneyrol, B., Forrester, D.I., Gardiner, B., González-Olabarria, J.R., Lyver, P.O., Meurisse, N., Oxbrough, A., Taki, H., Thompson, I.D., Van Der Plas, F., Jactel, H., 2017. Forest biodiversity, ecosystem functioning and the provision of ecosystem services. Biodivers. Conserv. 26, 3005–3035.
Cajander, A.K., 1909. Über Waldtypen. Acta Forestalia Fennica 1, 1–175.
Chraibi, E., De Boissieu, F., Barbier, N., Luque, S., Féret, J.-B., 2022. Stability in time and consistency between atmospheric corrections: Assessing the reliability of Sentinel-2 products for biodiversity monitoring in tropical forests. Int. J. Appl. Earth Obs. Geoinf. 112, 102884.
Coops, N.C., Tompalski, P., Goodbody, T.R.H., Achim, A., Mulverhill, C., 2023. Framework for near real-time forest inventory using multi source remote sensing data. Forestry: Int. J. Forest Res. 96, 1–19.
Daughtry, C.S.T., Serbin, G., Reeves, J.B., Doraiswamy, P.C., Hunt, E.R., 2010. Spectral reflectance of wheat residue during decomposition and remotely sensed estimates of residue cover. Remote Sens. (Basel) 2, 416–431.
Díaz-Yáñez, O., Pukkala, T., Packalen, P., Lexer, M.J., Peltola, H., 2021. Multi-objective forestry increases the production of ecosystem services. Forestry: Int. J. Forest Res. 94, 386–394.
Duarte, G.T., Ribeiro, M.C., Paglia, A.P., 2016. Ecosystem services modeling as a tool for defining priority areas for conservation. PLoS One 11, e0154573.
Erdenebaatar, N., Bayaraa, B., Damdinsuren, A., 2021. Application of Random Forest Approach to Biomass Estimation Using Remotely Sensed Data: Presented at the Environmental Science and Technology International Conference (ESTIC 2021), Ulaanbaatar, Mongolia.
Felipe-Lucia, M.R., Soliveres, S., Penone, C., Manning, P., Van Der Plas, F., Boch, S., Prati, D., Ammer, C., Schall, P., Gossner, M.M., Bauhus, J., Buscot, F., Blaser, S., Blüthgen, N., De Frutos, A., Ehbrecht, M., Frank, K., Goldmann, K., Hänsel, F., Jung, K., Kahl, T., Nauss, T., Oelmann, Y., Pena, R., Polle, A., Renner, S., Schloter, M., Schöning, I., Schrumpf, M., Schulze, E.-D., Solly, E., Sorkau, E., Stempfhuber, B., Tschapka, M., Weisser, W.W., Wubet, T., Fischer, M., Allan, E., 2018. Multiple forest attributes underpin the supply of multiple ecosystem services. Nat. Commun. 9, 4839.
Fu, B., Zhang, L., Xu, Z., Zhao, Y., Wei, Y., Skinner, D., 2015. Ecosystem services in changing land use. J. Soils Sediments 15, 833–843.
Gamfeldt, L., Snäll, T., Bagchi, R., Jonsson, M., Gustafsson, L., Kjellander, P., Ruiz-Jaen, M.C., Fröberg, M., Stendahl, J., Philipson, C.D., Mikusiński, G., 2013. Higher levels of multiple ecosystem services are found in forests with more tree species. Nat. Commun. 4 (1), 1340.
Gašparović, M., Medak, D., Pilaš, I., Jurjević, L., Balenović, I., 2018. Fusion of sentinel-2 and planetscope imagery for vegetation detection and monitoring. Int. Arch. Photogramm. Remote. Sens. Spat. Inf. Sci. 42, 155–160.
Giannetti, F., Chirici, G., Gobakken, T., Næsset, E., Travaglini, D., Puliti, S., 2018. A new approach with DTM-independent metrics for forest growing stock prediction using UAV photogrammetric data. Remote Sens. Environ. 213, 195–205.
Gitelson, A.A., Kaufman, Y.J., Merzlyak, M.N., 1996. Use of a green channel in remote sensing of global vegetation from EOS-MODIS. Remote Sens. Environ. 58, 289–298.
Hardisky, M.A., Daiber, F.C., Roman, C.T., Klemas, V., 1984. Remote sensing of biomass and annual net aerial primary productivity of a salt marsh. Remote Sens. Environ. 16, 91–106.
Hoffmann, J., Muro, J., Dubovyk, O., 2022. Predicting species and structural diversity of temperate forests with satellite remote sensing and deep learning. Remote Sens. (Basel) 14, 1631.
Hou, Z., Mehtätalo, L., McRoberts, R.E., Ståhl, G., Tokola, T., Rana, P., Siipilehto, J., Xu, Q., 2019. Remote sensing-assisted data assimilation and simultaneous inference for forest inventory. Remote Sens. Environ. 234, 111431.
Houborg, R., McCabe, M.F., 2018. A hybrid training approach for leaf area index estimation via Cubist and random forests machine-learning. ISPRS J. Photogramm. Remote Sens. 135, 173–188.
Huete, A.R., 1988. A soil-adjusted vegetation index (SAVI). Remote Sens. Environ. 25, 295–309.
Isoaho, A., Ikkala, L., Päkkilä, L., Marttila, H., Kareksela, S., Räsänen, A., 2024. Multi-sensor satellite imagery reveals spatiotemporal changes in peatland water table after restoration. Remote Sens. Environ. 306, 114144.
Jennings, S.B., Brown, N.D., Sheil, D., 1999. Assessing forest canopies and understorey illumination: canopy closure, canopy cover and other measures. Forestry 72 (1), 59–74.
Jia, H., Luo, P., Yang, H., Luo, C., Li, H., Wu, S., Cheng, Y., Huang, Y., Xie, W., 2022. Exploring the relationship between forest scenic beauty with color index and ecological integrity: case study of jiuzhaigou and giant panda national park in Sichuan. China. Forests 13, 1883.
Jiang, F., Deng, M., Tang, J., Fu, L., Sun, H., 2022. Integrating spaceborne LiDAR and Sentinel-2 images to estimate forest aboveground biomass in Northern China. Carbon Balance Manage 17, 12.
John, R., Chen, J., Giannico, V., Park, H., Xiao, J., Shirkey, G., Ouyang, Z., Shao, C., Lafortezza, R., Qi, J., 2018. Grassland canopy cover and aboveground biomass in Mongolia and Inner Mongolia: spatiotemporal estimates and controlling factors. Remote Sens. Environ. 213, 34–48.
Keränen, K., Isoaho, A., Räsänen, A., Hjort, J., Kumpula, T., Korpelainen, P., Rana, P., 2024. Multi-resolution remote sensing for flark area detection in boreal aapa mires. Int. J. Remote Sens. 45, 4324–4343.
Klein, T.M., Celio, E., Grêt-Regamey, A., 2015. Ecosystem services visualization and communication: a demand analysis approach for designing information and conceptualizing decision support systems. Ecosyst. Serv. 13, 173–183.
Kluczek, M., Zagajewski, B., Zwijacz-Kozica, T., 2023. Mountain tree species mapping using sentinel-2, PlanetScope, and airborne HySpex hyperspectral imagery. Remote Sens. (Basel) 15 (3), 844.
Korhonen, K., Ahola, A., Heikkinen, J., Henttonen, H., Hotanen, J.-P., Ihalainen, A., Melin, M., Pitkänen, J., Räty, M., Sirviö, M., Strandström, M., 2021. Forests of Finland 2014–2018 and their development 1921–2018. Silva Fenn. 55.
Korhonen, L., Hadi, P., Rautiainen, M., 2017. Comparison of Sentinel-2 and Landsat 8 in the estimation of boreal forest canopy cover and leaf area index. Remote Sens. Environ. 195, 259–274.
Korhonen, L., Peuhkurinen, J., Malinen, J., Suvanto, A., Maltamo, M., Packalen, P., Kangas, J., 2008. The use of airborne laser scanning to estimate sawlog volumes. Forestry 81, 499–510.
Krsnik, G., Reynolds, K.M., Murphy, P., Paplanus, S., Garcia-Gonzalo, J., González Olabarria, J.R., 2023. Forest use suitability: Towards decision-making-oriented sustainable management of forest ecosystem services. Geogr. Sustain. 4, 414–427.
Laasasenaho, J., 1982. Taper curve and volume functions for pine, spruce and birch, Communicationes Instituti Forestalis Fenniae. The Finnish Forest Research Institute, Helsinki.
Liang, X., Hyyppä, J., Matikainen, L., 2007. Deciduous-coniferous tree classification using difference between first and last pulse laser signatures. International Archives of Photogrammetry, Remote Sensing and Spatial. Inf. Sci. 36 (3/W52).
Liu, C.L.C., Kuchma, O., Krutovsky, K.V., 2018. Mixed-species versus monocultures in plantation forestry: development, benefits, ecosystem services and perspectives for the future. Global Ecol. Conserv. 15, e00419.
Liu, H.Q., Huete, A., 1995. A feedback based modification of the NDVI to minimize canopy background and atmospheric noise. IEEE Trans. Geosci. Remote Sens. 33, 457–465.
Lu, D., Chen, Q., Wang, G., Liu, L., Li, G., Moran, E., 2016. A survey of remote sensing-based aboveground biomass estimation methods in forest ecosystems. Int. J. Digital Earth 9, 63–105.

Mäkiranta, P., Laiho, R., Penttilä, T., Minkkinen, K., 2012. The impact of logging residue on soil GHG fluxes in a drained peatland forest. Soil Biol. Biochem. 48, 1–9.
Martínez-Harms, M.J., Balvanera, P., 2012. Methods for mapping ecosystem service supply: a review. Int. J. Biodiv. Sci., Ecosyst. Serv. & Manag. 8, 17–25.
McFeeters, S.K., 1996. The use of the Normalized Difference Water Index (NDWI) in the delineation of open water features. Int. J. Remote Sens. 17, 1425–1432.
MEA, 2005. Ecosystems and human well-being: wetlands and water synthesis : a report of the Millennium Ecosystem Assessment. World Resources Institute, Washington, DC.
Miina, J., Hotanen, J.-P., Salo, K., 2009. Modelling the abundance and temporal variation in the production of bilberry (Vaccinium myrtillus L.) in Finnish mineral soil forests. Silva Fenn. 43.
Minkkinen, K., Laine, J., Shurpali, N.J., Mäkiranta, P., Alm, J., Penttilä, T., 2007. Heterotrophic soil respiration in forestry-drained peatlands. Boreal Environ. Res. 12, 115–126.
Mononen, L., Vihervaara, P., Repo, T., Korhonen, K.T., Ihalainen, A., Kumpula, T., 2017. Comparative study on biophysical ecosystem service mapping methods—a test case of carbon stocks in Finnish Forest Lapland. Ecol. Ind. 73, 544–553.
Motohka, T., Nasahara, K.N., Oguma, H., Tsuchida, S., 2010. Applicability of green-red vegetation index for remote sensing of vegetation phenology. Remote Sens. (Basel) 2, 2369–2387.
Næsset, E., 2002. Predicting forest stand characteristics with airborne scanning laser using a practical two-stage procedure and field data. Remote Sens. Environ. 80, 88–99.
Nakano, T., Bavuudorj, G., Urianhai, N.G., Shinoda, M., 2013. Monitoring aboveground biomass in semiarid grasslands using MODIS images. J. Agric. Meteorol. 69, 33–39.
Näslund, M., 1936. Skogsförsöksanstaltens gallringsförsök i tallskog (in Swedish for "Forestry Institute's thinning trial in a pine forest"). Meddelanden från Statens skogsförsöksanstalt 29.
Orsi, F., Ciolli, M., Primmer, E., Varumo, L., Geneletti, D., 2020. Mapping hotspots and bundles of forest ecosystem services across the European Union. Land Use Policy 99, 104840.
Pacheco-Prado, D., Bravo-López, E., Ruiz, L.Á., 2024. Mapping polylepis forest using sentinel, planetscope images, and topographical features with machine learning. Remote Sens. (Basel) 16 (22).
Peura, M., Triviño, M., Mazziotta, A., Podkopaev, D., Juutinen, A., Mönkkönen, M., 2016. Managing boreal forests for the simultaneous production of collectable goods and timber revenues. Silva Fenn. 50.
Pope, G., Treitz, P., 2013. Leaf Area Index (LAI) estimation in boreal mixedwood forest of ontario, canada using light detection and ranging (LiDAR) and worldview-2 imagery. Remote Sens. (Basel) 5, 5040–5063.
Pukkala, T., 2016. Which type of forest management provides most ecosystem services? For. Ecosyst. 3, 9.
Pukkala, T., Kellomäki, S., Mustonen, E., 1988. Prediction of the amenity of a tree stand. Scand. J. For. Res. 3, 533–544.
Puliti, S., Breidenbach, J., Schumacher, J., Hauglin, M., Klingenberg, T.F., Astrup, R., 2021. Above-ground biomass change estimation using national forest inventory data with Sentinel-2 and Landsat. Remote Sens. Environ. 265, 112644.
Purohit, S., Aggarwal, S.P., Patel, N.R., 2021. Estimation of forest aboveground biomass using combination of Landsat 8 and Sentinel-1A data with random forest regression algorithm in Himalayan Foothills. Trop Ecol 62, 288–300.
Qiu, A., Yang, Y., Wang, D., Xu, S., Wang, X., 2020. Exploring parameter selection for carbon monitoring based on Landsat-8 imagery of the aboveground forest biomass on Mount Tai. Eur. J. Remote Sens. 53, 4–15.
Rana, M.P., 2016. Selection of training areas for remote sensing-based forest above-ground biomass estimation. Dissertationes Forestales. https://doi.org/10.14214/df.227.
Rana, P., Gautam, B., Tokola, T., 2016. Optimizing the number of training areas for modeling above-ground biomass with ALS and multispectral remote sensing in subtropical Nepal. Int. J. Appl. Earth Obs. Geoinf. 49, 52–62.
Rana, P., Popescu, S., Tolvanen, A., Gautam, B., Srinivasan, S., Tokola, T., 2023. Estimation of tropical forest aboveground biomass in Nepal using multiple remotely sensed data and deep learning. Int. J. Remote Sens. 44 (17), 5147–5171.
Rana, P., Vauhkonen, J., 2023. Stochastic multicriteria acceptability analysis as a forest management priority mapping approach based on airborne laser scanning and field inventory data. Landsc. Urban Plan. 230, 104637.
Räsänen, A., Wagner, J., Hugelius, G., Virtanen, T., 2021. Aboveground biomass patterns across treeless northern landscapes. Int. J. Remote Sens. 42, 4536–4561.
Raudsepp-Hearne, C., Peterson, G.D., Tengö, M., Bennett, E.M., Holland, T., Benessaiah, K., MacDonald, G.K., Pfeifer, L., 2010. Untangling the environmentalist's paradox: why is human well-being increasing as ecosystem services degrade? Bioscience 60, 576–589.
Reich, R.M., Lojewski, N., Lundquist, J.E., Bravo, V.A., 2018. Predicting abundance and productivity of blueberry plants under insect defoliation in Alaska. J. Sustain. For. 37, 525–536.
Rondeaux, G., Steven, M., Baret, F., 1996. Optimization of soil-adjusted vegetation indices. Remote Sens. Environ. 55, 95–107.
Rouse, J.W., Haas, R.H., Schell, J.A., Deering, D.W., 1974. Monitoring vegetation systems in the Great Plains with ERTS. NASA Spec. 351, 309.
Roy, D.P., Wulder, M.A., Loveland, T.R., C.E, W., Allen, R.G., Anderson, M.C., Helder, D., Irons, J.R., Johnson, D.M., Kennedy, R., Scambos, T.A., Schaaf, C.B., Schott, J.R., Sheng, Y., Vermote, E.F., Belward, A.S., Bindschadler, R., Cohen, W.B., Gao, F., Hipple, J.D., Hostert, P., Huntington, J., Justice, C.O., Kilic, A., Kovalskyy, V., Lee, Z. P., Lymburner, L., Masek, J.G., McCorkel, J., Shuai, Y., Trezza, R., Vogelmann, J., Wynne, R.H., Zhu, Z., 2014. Landsat-8: Science and product vision for terrestrial global change research. Remote Sens. Environ. 145, 154–172.
Saarikoski, H., Jax, K., Harrison, P.A., Primmer, E., Barton, D.N., Mononen, L., Vihervaara, P., Furman, E., 2015. Exploring operational ecosystem service definitions: the case of boreal forests. Ecosyst. Serv. 14, 144–157.
Savolainen, R., Kellomaki, S., 1981. Scenic value of forest landscape. Acta Forestalia Fennica 170, 74.
Schirpke, U., Tasser, E., Tappeiner, U., 2013. Predicting scenic beauty of mountain regions. Landsc. Urban Plan. 111, 1–12.
Shen, X., Cao, L., Yang, B., Xu, Z., Wang, G., 2019. Estimation of Forest Structural Attributes Using Spectral Indices and Point Clouds from UAS-Based Multispectral and RGB Imageries. Remote Sens. (Basel) 11, 800.
Tuominen, S., Pitkänen, T., Balazs, A., Kangas, A., 2017. Improving finnish multi-source national forest inventory by 3D aerial imaging. Silva Fenn. 51.
Vauhkonen, J., 2018. Predicting the provisioning potential of forest ecosystem services using airborne laser scanning data and forest resource maps. For. Ecosyst. 5, 24.
Vauhkonen, J., Imponen, J., 2016. Unsupervised classification of airborne laser scanning data to locate potential wildlife habitats for forest management planning. Forestry 89, 350–363.
Vauhkonen, J., Ruotsalainen, R., 2017. Assessing the provisioning potential of ecosystem services in a Scandinavian boreal forest: suitability and tradeoff analyses on grid-based wall-to-wall forest inventory data. For. Ecol. Manage. 389, 272–284.
Wang, C., Chen, J., Wu, J., Tang, Y., Shi, P., Black, T.A., Zhu, K., 2017. A snow-free vegetation index for improved monitoring of vegetation spring green-up date in deciduous ecosystems. Remote Sens. Environ. 196, 1–12.
Wang, M., Zheng, Y., Huang, C., Meng, R., Pang, Y., Jia, W., Zhou, J., Huang, Z., Fang, L., Zhao, F., 2022. Assessing Landsat-8 and Sentinel-2 spectral-temporal features for mapping tree species of northern plantation forests in Heilongjiang Province. China. Forest Ecosystems 9, 100032.
Wang, Z., Li, M., Zhang, X., Song, L., 2020. Modeling the scenic beauty of autumnal tree color at the landscape scale: a case study of Purple Mountain, Nanjing. China. Urban Forestry & Urban Greening 47, 126526.
Wittke, S., Yu, X., Karjalainen, M., Hyyppä, J., Puttonen, E., 2019. Comparison of two-dimensional multitemporal Sentinel-2 data with three-dimensional remote sensing data sources for forest inventory parameter estimation over a boreal forest. Int. J. Appl. Earth Obs. Geoinf. 76, 167–178.
Wulder, M.A., Loveland, T.R., Roy, D.P., Crawford, C.J., Masek, J.G., Woodcock, C.E., Allen, R.G., Anderson, M.C., Belward, A.S., Cohen, W.B., Dwyer, J., 2019. Current status of Landsat program, science, and applications. Remote Sens. Environ. 225, 127–147.
Zhang, Y., Wang, N., Wang, Y., Li, M., 2023. A new strategy for improving the accuracy of forest aboveground biomass estimates in an alpine region based on multi-source remote sensing. Gisci. Remote Sens. 60, 2163574.